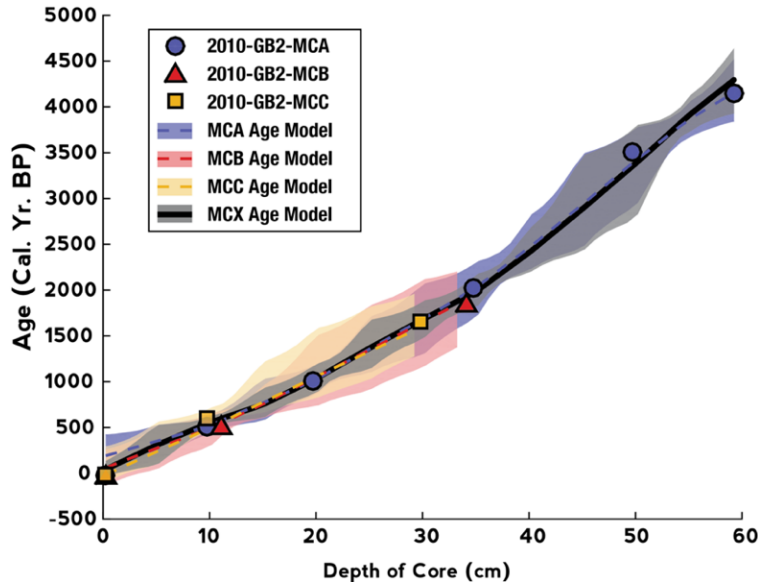


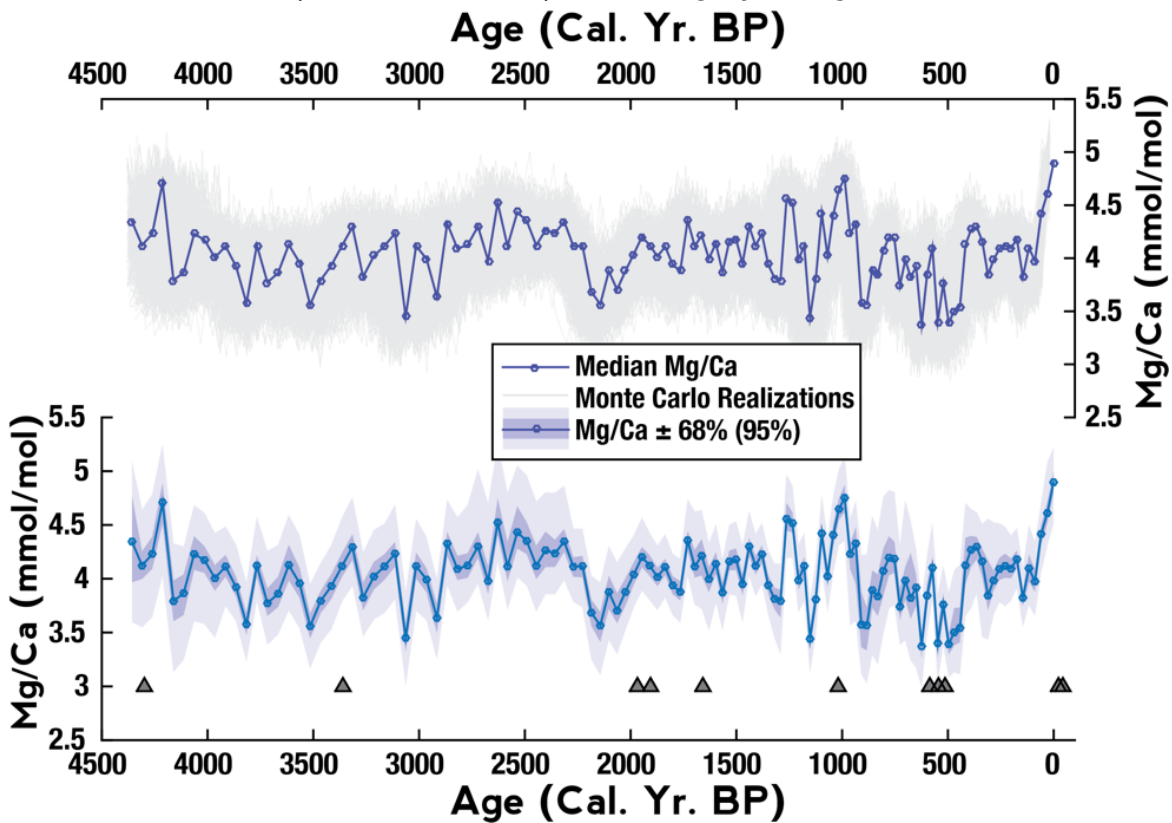
## Supplementary Figures



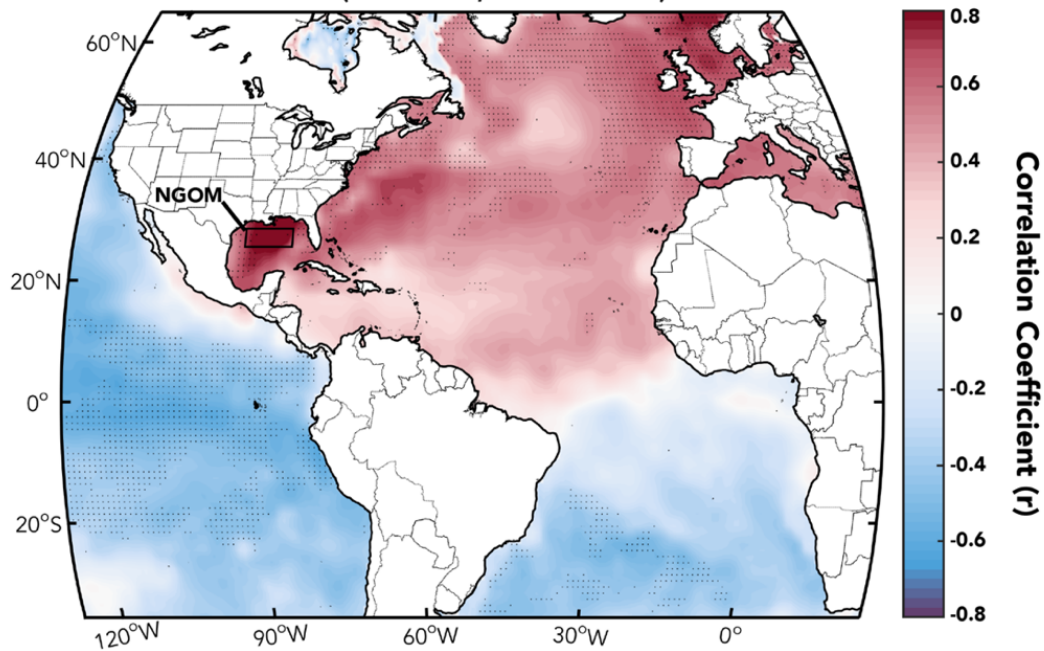
**Supplementary Figure 1.**

Bayesian posteriors of calibrated ages versus depth for MCA (purple), MCB (red), MCC (yellow), and the overall age model (MCX; black) using BACON<sup>1</sup>. The full uncertainty envelopes have been plotted.

**Supplementary Figure 2.** A demonstration of our uncertainty modeling algorithm where 5000 Mg/Ca time series from MCA are plotted using a bootstrap Monte Carlo framework. We plot the median value and associated 68% and 95% confidence bounds in the second panel. Dates are plotted in grey triangles below.

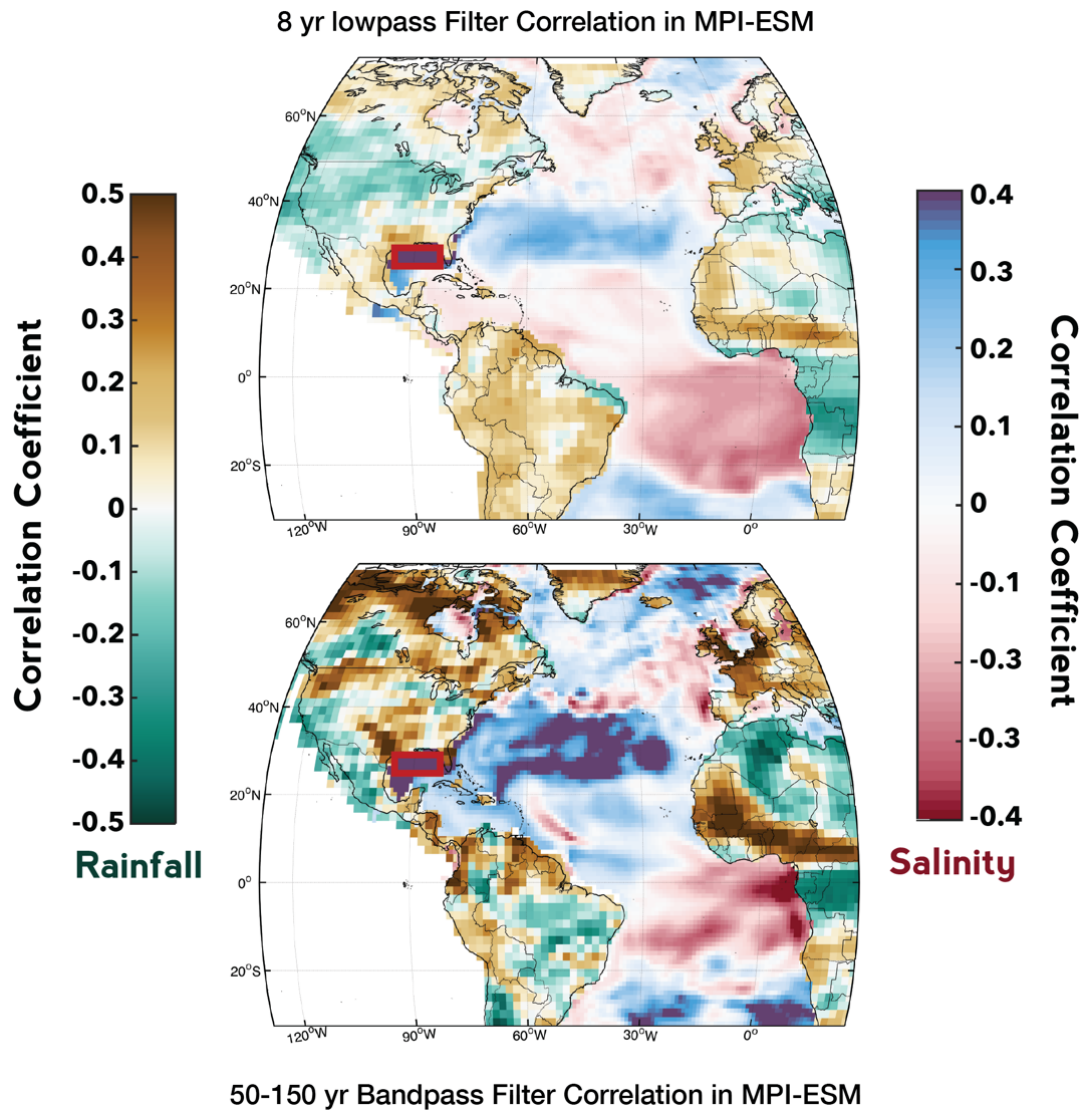


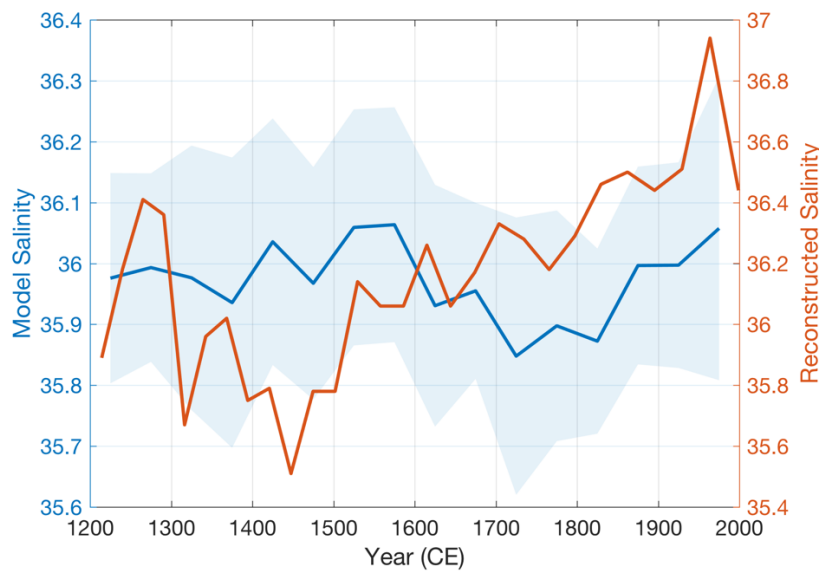
NGOM-SST Multidecadal Correlation  
(HadISST, 1870-2015)



**Supplementary Figure 3.** Correlation map between northern Gulf of Mexico SSTs (black box) and global oceanic SST using the gridded HadISST monthly dataset. The data were filtered using an 8-year Gaussian filter and detrended prior to correlation to reduce sensitivity to interannual variability. Stippling indicates significance at the 95% level. The map in this figure was generated using the *M\_MAP* package in MATLAB.

**Supplementary Figure 4.** Comparison between correlation analyses performed on MPI-ESM last millennium output using an 8-yr lowpass filter and the 50-150-yr bandpass filter. Correlation analyses were performed as described in the Methods section. Maps in this figure were generated using the *M\_MAP* package in MATLAB.





**Supplementary Figure 5.** For illustrative purposes: comparison between the low-frequency (50-yr running mean with standard error; blue) simulated salinity in the northern Gulf of Mexico over the last millennium from the MPI-ESM and the reconstructed salinity (orange) at the Garrison Basin site.

---

## Supplementary Table

**Supplementary Table 1.** List of proxies utilized in Figure 1. LIA-mean calculated based on mean state during LIA (1450-1850 AD) relative to the modern era.

Location	Proxy Type	Expectation during LIA based on observations*	Proxy Record during LIA†
<b>Salinity Proxies</b>			
Garrison Basin, GOM	<i>G. ruber</i> (W) $\delta^{18}\text{O}_{\text{sw}}$	Fresher	Fresher
Pigmy Basin <sup>2</sup> , GOM	<i>G. ruber</i> (W) $\delta^{18}\text{O}_{\text{sw}}$	Fresher	Fresher
Dry Tortugas <sup>3</sup>	<i>G. ruber</i> (W) $\delta^{18}\text{O}_{\text{sw}}$	Fresher	Fresher
Great Bahama Bank <sup>3</sup>	<i>G. ruber</i> (W) $\delta^{18}\text{O}_{\text{sw}}$	Fresher	Fresher
Carolina Slopes <sup>4</sup>	<i>G. ruber</i> (W) $\delta^{18}\text{O}_{\text{sw}}$	Fresher	Fresher
Bermuda <sup>5</sup>	<i>D. labyrinthiformis</i> $\delta^{18}\text{O}_{\text{sw}}$	Fresher	Fresher
Puerto Rico <sup>6</sup>	<i>M. faveolata</i> $\delta^{18}\text{O}_{\text{sw}}$	Fresher	Fresher
Feni Drift <sup>7</sup>	<i>G. bulloides</i>	Fresher	Saltier
South Iceland Rise <sup>8</sup>	<i>G. bulloides</i>	Fresher/No Change	No Change
Labrador Sea <sup>9</sup>	<i>T. quinqueloba</i> $\delta^{18}\text{O}_{\text{sw}}$	Fresher	Fresher
<b>Precipitation Proxies</b>			
Ghana <sup>10</sup>	Authigenic Carbonate $\delta^{18}\text{O}$	Dryer	Dryer
Cariaco Basin <sup>11</sup>	Titanium Percent	Dryer	Dryer
Peruvian Andes <sup>12</sup>	Authigenic Carbonate $\delta^{18}\text{O}$	Wetter	Wetter
Quelcayya Ice Cap <sup>13</sup>	Ice Core $\delta^{18}\text{O}$	Wetter	Wetter
Northern Peru <sup>14</sup>	Stalagmite $\delta^{18}\text{O}$	Wetter	Wetter
Northwestern Venezuela <sup>15</sup>	Cyperaceae Pollen, Magnetic Susceptibility	Wetter	Wetter
Central Mexico <sup>16</sup>	Stalagmite $\delta^{18}\text{O}$	Wetter	Wetter

Central Mexico <sup>17</sup>	Authigenic Carbonate $\delta^{18}\text{O}$	Wetter	Wetter
Yucatan <sup>18</sup>	Stalagmite $\delta^{18}\text{O}$	Wetter	Wetter
Southwest US <sup>19</sup>	Tree-rings	Wetter	Wetter
New Mexico <sup>20</sup>	Stalagmite Width	Wetter	Wetter
Southeast US <sup>19</sup>	Tree-rings	Dryer	Dryer

\* - Based on Figure 1 correlation analysis

† - Calculated based on the difference in mean of  $\delta^{18}\text{O}_{\text{sw}}$  record from 1450-1850 C.E. and mean from 1850 C.E.-present(/coretop).

## Supplementary References

1. Blaauw, M. & Christen, J. A. Flexible Paleoclimate Age-Depth Models Using an Autoregressive Gamma Process. *Bayesian Analysis* **6**, 457-474 (2011).
2. Richey, J. N., Poore, R. Z., Flower, B. P. & Quinn, T. M. 1400 yr multiproxy record of climate variability from the northern Gulf of Mexico. *Geol.* **35**, 423-4 (2007).
3. Lund, D. C. & Curry, W. B. Florida Current surface temperature and salinity variability during the last millennium. *Paleoceanography* **21**, PA2009-15 (2006).
4. Saenger, C., Came, R. E., Oppo, D. W., Keigwin, L. D. & Cohen, A. L. Regional climate variability in the western subtropical North Atlantic during the past two millennia. *Paleoceanography* **26**, PA2206 (2011).
5. Goodkin, N. F., Hughen, K. A., Curry, W. B., Doney, S. C. & Ostermann, D. R. Sea surface temperature and salinity variability at Bermuda during the end of the Little Ice Age. *Paleoceanography* **23**, PA3203 (2008).
6. Kilbourne, K. H. *et al.* Coral windows onto seasonal climate variability in the northern Caribbean since 1479. *Geochem. Geophys. Geosyst.* **11**, n/a-n/a (2010).
7. Richter, T. O., Peeters, F. J. C. & van Weering, T. C. E. Late Holocene (0-2.4kaBP) surface water temperature and salinity variability, Feni Drift, NE Atlantic Ocean. *Quat. Sci. Rev.* **28**, 1941-1955 (2009).
8. Thornalley, D. J. R., Elderfield, H. & McCave, I. N. Holocene oscillations in temperature and salinity of the surface subpolar North Atlantic. *Nature* **457**, 711-714 (2009).
9. Moffa-Sanchez, P., Hall, I. R., Barker, S., Thornalley, D. J. R. & Yashayaev, I. Surface changes in the eastern Labrador Sea around the onset of the Little Ice Age. *Paleoceanography* **29**, 160-175 (2014).
10. Shanahan, T. M. *et al.* Atlantic Forcing of Persistent Drought in West Africa.

- Science* **324**, 1-4 (2009).
11. Haug, G. H., Hughen, K. A., Sigman, D. M., Peterson, L. C. & Röhl, U. Southward Migration of the Intertropical Convergence Zone Through the Holocene. *Science* **293**, 1304-1308 (2001).
  12. Bird, B. W., Abbott, M. B. & Vuille, M. A 2,300-year-long annually resolved record of the South American summer monsoon from the Peruvian Andes. *Proc. Nat. Acad. Sci.* **108**, 8583-8588 (2011).
  13. Thompson, L. G., Mosley-Thompson, E., Dansgaard, W. & Grootes, P. M. The Little Ice Age as Recorded in the Stratigraphy of the Tropical Quelccaya Ice Cap. *Science* **234**, 361-364 (1986).
  14. Reuter, J. *et al.* A new perspective on the hydroclimate variability in northern South America during the Little Ice Age. *Geophys. Res. Lett.* **36**, L21706-5 (2009).
  15. Polissar, P. J. *et al.* Solar modulation of Little Ice Age climate in the tropical Andes. *Proc. Nat. Acad. Sci.* **103**, 8937-8942 (2006).
  16. Lachniet, M. S., Bernal, J. P., Asmerom, Y., Polyak, V. J. & Piperno, D. R. A 2400 yr Mesoamerican rainfall reconstruction links climate and cultural change. *Geol.* **40**, 259-262 (2012).
  17. Bhattacharya, T. *et al.* Cultural implications of late Holocene climate change in the Cuenca Oriental, Mexico. *Proc. Nat. Acad. Sci.* **112**, 1693-1698 (2015).
  18. Medina-Elizalde, M. & Rohling, E. J. Collapse of Classic Maya Civilization Related to Modest Reduction in Precipitation. *Science* **335**, 956-959 (2012).
  19. Cook, E. R., Seager, R., Cane, M. A. & Stahle, D. W. North American drought: Reconstructions, causes, and consequences. *Earth Sci. Rev.* **81**, 93-134 (2007).
  20. Polyak, V. J. & Asmerom, Y. Late Holocene Climate and Cultural Changes in the Southwestern United States. *Science* **294**, 148-151 (2001).